Estimation of temporal separation of slow light pulses in atomic vapors by weak measurement

Pardeep Kumar* and Shubhrangshu Dasgupta
Department of Physics, Indian Institute of Technology Ropar, Rupnagar, Punjab 140001, India
(Received 1 December 2014; published 3 April 2015)

We show how two circular polarization components of a linearly polarized pulse, propagating through a coherently driven dilute atomic vapor, can be well resolved in a time domain by weak measurement. The slower group velocity of one of the components due to electromagnetically induced transparency leads to a differential group delay between the two components. For a low number density, this delay may not be large enough to temporally resolve the two components. We show how this can be enhanced in terms of the mean time of arrival of the output pulse through a postselected polarizer. We demonstrate the idea with all the analytical and numerical results, with a specific example of alkali atoms.

DOI: 10.1103/PhysRevA.91.043803 PACS number(s): 42.50.Gy, 42.25.Kb, 03.65.Ta

I. INTRODUCTION

It is known from the measurement theory that measurement of an observable of the system over a long period of time leads to a statistical average of all the output results put together (called "the expectation value" of the observable). This is valid irrespective of the interaction strength between the system and the measuring device. However, in the case of weak interaction, contrary to strong interaction, the system does not collapse into one of the eigenstates of the observable, leading to a large uncertainty at the output. In such a case, a large "weak value" of the observable can be obtained, if one considers only a postselected set of the output results. Such a postselection of the basis for strong measurement immediately after weak interaction makes an essential component of the weak measurement procedure which was proposed in [1] by Aharonov, Albert, and Vaidman and further investigated in [2–4]. The technique of weak measurement was first demonstrated in an optical experiment by Ritchie *et al.* [5]. Weak value has been demonstrated to be useful in small parameter estimation, e.g., in resolving Angstrom-scale optical beam deflection [6,7], frequency shifts [8], phase shifts [9], temporal shifts, [10,11] and temperature shifts [12]. It has also been employed in the direct measurement of quantum states [13–15]. A nice review on weak measurement can be found in [16]. Recently, the weak measurements are also proposed in quantum dots [17,18].

Previous demonstrations of weak measurement in optical experiments [5,6,8–11] can be explained semiclassically using a wave equation derived from Maxwell's equations. Recently, the experiments have been proposed [19–22] and demonstrated [23–25] which can be explained with a quantum mechanical perspective. In [23], an entangling circuit has been shown to enable one single photon to make weak measurement of the polarization of the other. Further, weak values of the observables using entangled photons in parametric down-conversion have been explored in [19]. A method to generate two qubit entanglement in a controlled way, using weak measurements, has been proposed in [20]. The quantum mechanical explanation for the interferometric weak value deflections [7] has been given in [25]. Wang *et al.* [24] have presented an experiment to measure the weak values of the arrival time of a single photon, by using the proposal of Ahnert and Payne [22].

The usefulness of weak values has also been perfectly demonstrated in the superluminal propagation of a charged particle [26] and by electromagnetic pulse propagation [27,28]. Solli *et al.* [27], in the experiment with polarized *microwaves* and two-dimensional birefringent *photonic crystals*, have derived a complex relation between a system's response function and the weak values of the polarization of the photon. On the other hand, in an experiment with *optical pulses* in *optical fiber*, Brunner *et al.* [28,29] have shown that a weak value of polarization can also be related to the mean time of arrival ($\langle t \rangle$) of the pulse in a postselected polarization, as

$$\langle t \rangle = \frac{\delta\tau}{2} \mathrm{Re}\langle \sigma_z \rangle_w, \tag{1}$$

where $\delta\tau$ is the differential group delay (DGD), i.e., the temporal separation between the pulse peaks of the polarization modes ($|H\rangle$,$|V\rangle$), which are eigenstates of the operator σ_z: $\sigma_z|H\rangle = |H\rangle$ and $\sigma_z|V\rangle = -|V\rangle$. Here,

$$\mathrm{Re}\langle \sigma_z \rangle_w = \mathrm{Re}\left[\frac{\langle \psi_f|\sigma_z|\psi_i\rangle}{\langle \psi_f|\psi_i\rangle}\right] \tag{2}$$

is the real part of the weak value (w signifies the weak value) of the polarization observable when it is measured between a preselected state $|\psi_i\rangle$ and a postselected state $|\psi_f\rangle$.

In this paper, we employ the above concept of mean time of arrival and weak value [Eq. (1)] to an *optical pulse* with preselected polarization, propagating through the *atomic vapor systems* [30,31]. Such systems, with suitable atomic configuration and in the presence of a strong coherent field, can act as a polarization splitter of pulses [32]. This happens when two polarization components propagate through the atomic medium with negligible absorption, but with different group velocities. We show, if the two circularly polarized components of a linearly polarized probe pulse are not well resolved in the time domain, their temporal separation $\delta\tau$ can be indirectly inferred by measuring the mean time of arrival $\langle t \rangle$ of a postselected pulse. Note that $\langle t \rangle$ can be made much larger than $\delta\tau$ by a suitable choice of the postselected basis. Therefore, the output pulse can be well resolved from the reference input pulse. We further obtain a one-to-one correspondence between $\delta\tau$ and $\langle t \rangle$ over a large range of the control parameters. Such

*pradeep.kumar@iitrpr.ac.in

a kind of correspondence can be used to obtain the number density N of the atomic medium, as well. Note that such an idea was employed in [28] to temporally resolve two photon pulses in optical fibers and indirectly calculate their superluminal velocities, while in this paper, we demonstrate this using slow optical pulses propagating through coherently driven atomic vapors. In addition, we can also coherently control the time separation $\delta\tau$ and therefore the weak values, a feature that is inherently absent in optical fibers. It is to be noted here that a semiclassical treatment is sufficient to explain the results presented in this paper.

The structure of the paper is as follows. In Sec. II, we theoretically study the temporal separation between the circular components of the probe pulse via weak measurements, which can be found through appropriate preselected and postselected states of the system. In this section the main results of the paper are presented. Section III contains the discussion and concluding remarks.

II. WEAK MEASUREMENT IN ATOMIC VAPORS

Three necessary steps for weak measurements are: (1) preselection of a quantum state; (2) weak interaction between the system and the measuring device; and (3) postselection of a quantum state. We consider weak measurement of the polarization of an optical pulse and that the energy of the pulse takes the role of the measuring device. We describe below how this measurement can be done using the three essential steps mentioned above.

A. Preselection of polarization

We consider the propagation of a linearly polarized input probe pulse through an atomic medium (with two ground states $|1\rangle$ and $|2\rangle$ and two excited states $|3\rangle$ and $|4\rangle$; see the Appendix for a detailed discussion) of length L. The input pulse propagating along z direction can be written in terms of its Fourier components as

$$\vec{E}(z,t) = \hat{x}\int_{-\infty}^{+\infty}\varepsilon(\omega)\exp\left\{i\omega\left(\frac{z}{c}-t\right)\right\}d\omega + \text{c.c.}, \quad (3)$$

where $\varepsilon(\omega)$ is the amplitude of the profile of the pulse. Here $\hat{x}$ denotes the polarization state of the probe pulse and can be written as

$$|\psi_o\rangle = \frac{1}{\sqrt{2}}(|\sigma_+\rangle + |\sigma_-\rangle), \quad (4)$$

which is equivalent to the preselection of polarization. Note that the circular polarization states $(|\sigma_+\rangle,|\sigma_-\rangle)$ make the eigenbasis of the Pauli spin matrix σ_y: $\sigma_y|\sigma_\pm\rangle = \pm|\sigma_\pm\rangle$.

In presence of the control field, these two polarization components propagate with different group velocities through the atomic medium. This can be explained as follows. When the central frequency of the probe pulse is in near resonance with the $|4\rangle \leftrightarrow |1\rangle$ transition, the control field, resonant with the $|4\rangle \leftrightarrow |2\rangle$ transition, makes an electromagnetically induced transparency (EIT) window for the σ_- polarization component. This is also associated with a large normal dispersion and hence a slow group velocity of this component. A magnetic field can be applied to remove the degeneracy of the ground and the excited state manifold. This makes the σ_+ component far from resonance from the $|3\rangle \leftrightarrow |2\rangle$ transition. Therefore the dispersion profile for this component exhibits a much flatter behavior in the frequency domain, leading to its group velocity being not too different from c, the velocity of light in a vacuum. Because of the difference in the group velocities inside the medium, the two circularly polarized components come out of the medium at different times with negligible absorption. In this way, the medium temporally separates the two orthogonal polarization components of the input pulse.

B. Weak interaction

In this paper, we focus on a situation where the temporal separation $\delta\tau$ between circular polarized components is much smaller than the width of the pulse such that the detector cannot resolve between these two components in the time domain, i.e., $\delta\tau < \Delta t$, Δt being the temporal resolution of the detector. Because, the group velocities are proportional to the number density N of the atomic medium, such a situation would arise when N is sufficiently small. In this paper, we consider $N = 10^9$ cm^{-3}. Note that this situation mimics a weak interaction between the light pulse and the atomic medium, that plays the role of a measuring device for the polarization state of the pulse.

For negligible absorption, the weak interaction gives rise to a rotation of the polarization of the input field of frequency ω_0 and the polarization state of the output field would read as [28]

$$|\phi\rangle = \frac{1}{\sqrt{2}}[e^{i\delta\tau\omega_o/2}|\sigma_+\rangle + e^{-i\delta\tau\omega_o/2}|\sigma_-\rangle]. \quad (5)$$

In the present case, to demonstrate the weak interaction, we choose the following Gaussian profile for the input pulse [Eq. (3)], as shown in Fig. 1(a):

$$\varepsilon(\omega) = \varepsilon_0\frac{1}{\sigma\sqrt{\pi}}\exp[-\omega^2/\sigma^2]; \varepsilon(t) = \varepsilon_0\frac{1}{\sqrt{2\pi}}\exp\left[-\sigma_t^2 t^2\right], \quad (6)$$

where σ ($\sigma_t = 2/\sigma$) is the width of the Gaussian pulse in the frequency (time) domain and ε_0 is the pulse amplitude.

The weak interaction of the linearly polarized probe pulse induces the following polarization in the medium

$$\vec{P}(z,t) = P_+(z,t)|\sigma_+\rangle + P_-(z,t)|\sigma_-\rangle, \quad (7)$$

where

$$P_\pm(z,t) = \int_{-\infty}^{+\infty}\chi_\pm(\omega)\varepsilon(z,\omega)e^{-i\omega t}d\omega. \quad (8)$$

Here $\chi_\pm(\omega)$ are the complex susceptibilities of the atomic medium corresponding to the $\sigma_\pm$ components and can be calculated using Eqs. (A10) and (A11) in the Appendix. Further $\varepsilon_\pm(\omega) = \frac{\varepsilon(\omega)}{\sqrt{2}}$ are the amplitudes for the $\sigma_\pm$ components and $\varepsilon(\omega)$ is given by Eq. (6).

The polarization state of the output field (at $z = L$) after the weak interaction reads as

$$|\psi\rangle = E_+(t)|\sigma_+\rangle + E_-(t)|\sigma_-\rangle, \quad (9)$$

where

$$E_\pm(t) = \int_{-\infty}^{+\infty}d\omega\varepsilon_\pm(\omega)\exp\left\{i\omega\left(\frac{L}{c}-t\right) + \frac{2\pi i\omega L}{c}\chi_\pm(\omega)\right\}. \quad (10)$$

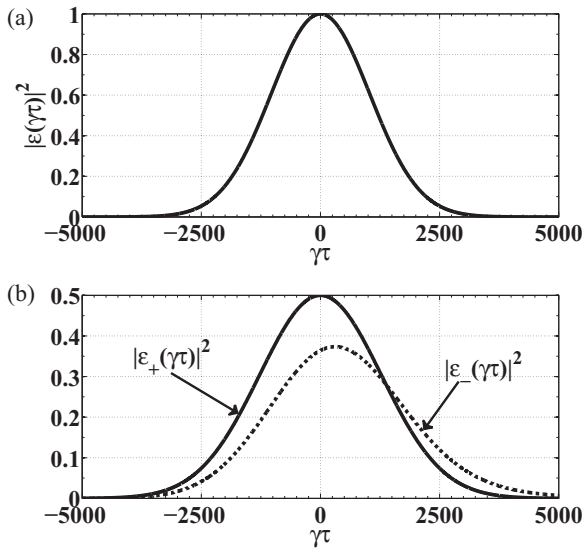

FIG. 1. (a) The normalized input Gaussian pulse in the time domain with a width of $\sigma_t = 400\ \mu$s ($\sigma = 2\pi \times 0.7916$ kHz) (b) The normalized circular polarization components [σ_+ (solid line) and σ_- (dotted line)] at the output of the medium. We choose the following parameters: $N = 10^9$ atoms cm^{-3}, the length of the medium $L = 1$ cm, the central wavelength of the input pulse $\lambda = 769.9$ nm, the spontaneous emission rate $A = 2\pi \times 6.079$ MHz, pertaining to ^{39}K atoms, $\gamma = \frac{A}{6}$, $B = 5\gamma$, $\gamma_{13} = \gamma_{24} = \gamma$, $\gamma_{23} = \gamma_{14} = 2\gamma$, $\gamma_{\rm coll} = 0$, $\Gamma_{32} = \Gamma_{31} = \Gamma_{41} = \Gamma_{42} = \frac{3}{2}\gamma$, $\Gamma_{43} = 3\gamma$, $\Gamma_{21} = \gamma_{\rm coll}$, $G = 0.03\gamma$, and $\tau = t - L/c$.

Note that the pulse suffers finite absorption (though small due to the EIT condition for the σ_- component and the off-resonance of the other), contrary to the case of optical fiber, which would gives rise to the polarization as described in Eq. (5).

We display in Fig. 1(b) the output intensities of both the polarization components. It is evident that these two components are not well resolved in the time domain. We find the temporal separation to be $\delta\tau = 305/\gamma$, while the pulse width in the time domain is $\sigma_t = 2520/\gamma$ ($\gg\delta\tau$). It is clear that one of the polarization components suffers absorption.

C. Postselection of polarization

The final and most important step of the weak measurement is a postselection of measurement basis. This is equivalent to using a polarizer with a suitable orientation at the output. We choose the following postselected polarization basis:

$$|\psi_1\rangle = \cos\left(\frac{\pi}{4} - \beta\right)|\sigma_+\rangle - \sin\left(\frac{\pi}{4} - \beta\right)|\sigma_-\rangle, \tag{11}$$

where $0 < \beta \ll 1$. This makes $|\psi_1\rangle$ nearly orthogonal to $|\psi_o\rangle$. The schematic optical setup of all the above three essential steps of weak measurement is shown in Fig. 2.

The temporal shape of the output pulse through this polarizer can thus be written as

$$\vec{E}_{\rm out}(t) = \left[\cos\left(\frac{\pi}{4} - \beta\right)\langle\sigma_+| - \sin\left(\frac{\pi}{4} - \beta\right)\langle\sigma_-|\right] \cdot[E_+(t)|\sigma_+\rangle + E_-(t)|\sigma_-\rangle]. \tag{12}$$

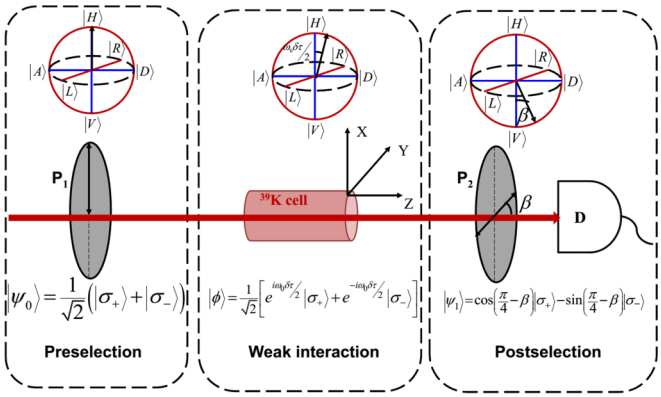

FIG. 2. (Color online) Schematic diagram of the setup. Polarizer P_1 performs the preselection of the polarization state, polarizer P_2 performs the postselection, and D is the detector. Poincaré spheres represent the polarization states of the fields at each stage.

Therefore the output intensity $I_{\rm out}(t) = |\vec{E}_{\rm out}(t)|^2$ reads as

$$I_{\rm out}(t) = |E_+(t)|^2\cos^2\left(\frac{\pi}{4} - \beta\right) + |E_-(t)|^2\sin^2\left(\frac{\pi}{4} - \beta\right) - 2{\rm Re}(E_+^*(t)E_-(t))\sin\left(\frac{\pi}{4} - \beta\right)\cos\left(\frac{\pi}{4} - \beta\right), \tag{13}$$

where $|E_\pm(t)|^2$ correspond to the Gaussian profiles for the $|\sigma_\pm\rangle$ components. Note that the strong interaction refers to the fact that two polarization components are well resolved, i.e., $\delta\tau \gg \sigma$. This is because, the interference term in Eq. (13) almost vanishes at this limit, i.e., $E_+^*(t)E_-(t) \approx 0$. But for the case of weak interaction, $\delta\tau \ll \sigma$, the two Gaussian pulses overlap as shown in Fig. 1(b) and the contribution of the interference term to the output intensity is no longer negligible. This leads to a very different temporal profile of the output pulse, as discussed below.

D. Temporal separation in terms of weak values

To obtain temporal separation for these two overlapping pulses at the output, we make use of the weak value of the polarization, defined as [29],

$$W = \frac{\langle\psi_1|\sigma_y|\psi\rangle}{\langle\psi_1|\psi\rangle}. \tag{14}$$

As seen from Eq. (14), W can be made arbitrarily large by choosing the state $|\psi\rangle$ and $|\psi_1\rangle$ nearly orthogonal, i.e., $\langle\psi_1|\psi\rangle \approx 0$. This weak value is related with mean time of arrival through Eq. (1), that can be calculated through the following relation:

$$\langle t\rangle = \frac{\int t\, I_{\rm out}dt}{\int I_{\rm out}dt}. \tag{15}$$

Using (9), (11), and (14), we have

$${\rm Re}W = \frac{\cot(\beta)}{\cos^2\left(\frac{\omega_0\delta\tau}{2}\right) + \cot^2(\beta)\sin^2\left(\frac{\omega_0\delta\tau}{2}\right)}. \tag{16}$$

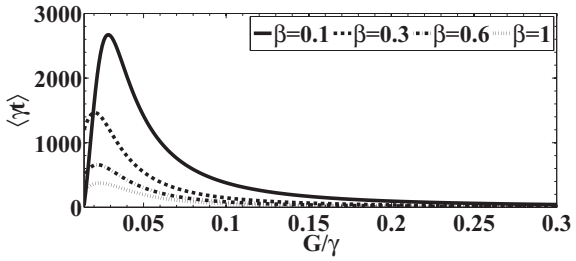

FIG. 3. Variation of the mean time of arrival with G/γ for different values of β. Other parameters are the same as in Fig. 1.

From (1), we finally obtain the following relation between $\delta\tau$ and $\langle t\rangle$:

$$\langle t\rangle = \frac{\delta\tau}{2}\mathrm{Re}\langle\sigma_y\rangle_w = \frac{\delta\tau}{2}\frac{\cot(\beta)}{\cos^2\left(\frac{\omega_0\delta\tau}{2}\right)+\cot^2(\beta)\sin^2\left(\frac{\omega_0\delta\tau}{2}\right)}. \tag{17}$$

With increase in the Rabi frequency $2G$ of the control field, the slope of the dispersion profile decreases, leading to a decrease (towards c) in the group velocity of the σ_- polarization component. Therefore, the temporal separation $\delta\tau$ between the σ_+ and σ_- components decreases. In this regime, the denominator of Eq. (17) approaches unity and the mean time of arrival becomes $\langle t\rangle \approx \frac{\delta\tau}{2}\cot(\beta)$.

As we choose $\beta \ll 1$, the above discussion suggests that $\langle t\rangle$ can be made much larger than $\delta\tau$. Thus, the temporal separation can be inferred indirectly by measuring the mean time of arrival of the output pulse through a postselected polarizer. This is possible by carefully choosing the relative orientation of the preselected and the postselected polarizer, i.e., by suitably choosing β. It can be observed from Fig. 3 that at $\beta = 0.1$, the mean time of arrival attains the highest value. We choose $\beta = 0.1$ in the rest of the paper.

Further, a one-to-one correspondence between $\delta\tau$ and $\langle t\rangle$ is evident by comparing Figs. 3 and 4. For a given value of G/γ, the value of $\langle\gamma t\rangle$ and the corresponding value of the temporal separation $\gamma\delta\tau$ can be inferred from Figs. 3 and 4. We demonstrate this correspondence in Fig. 5 where we show how $2\langle\gamma t\rangle$ varies linearly with $\gamma\delta\tau$. In this linear regime, the absorption of the two polarization components is negligible and the slope of this linearity is approximately equal to $\frac{\cot\beta}{2}$. Note that in the nonlinear regime, $\langle\gamma t\rangle$ depends nontrivially on G/γ [in addition to β; see Eq. (17)] and thus the control field provides an extra handle in measuring $\langle\gamma t\rangle$.

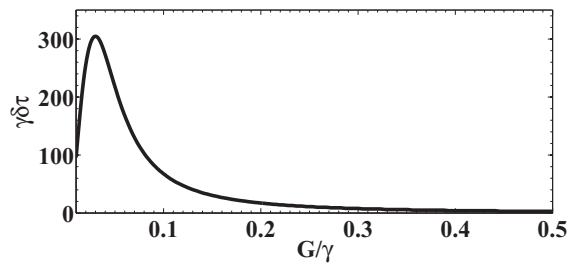

FIG. 4. The variation of the differential group delay ($\gamma\delta\tau$) with G/γ. The other parameters are the same as in Fig. 3.

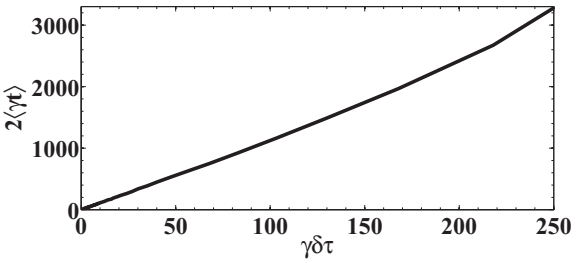

FIG. 5. The variation of $2\langle\gamma t\rangle$ with $\gamma\delta\tau$. The parameters used here are the same as in Fig. 4.

We demonstrate in Fig. 6 how the use of a postselected polarizer with $\beta = 0.1$ leads to a large temporal shift of the output pulse, compared to the input reference pulse (the peak-to-peak separation between these two pulses is found to be $2618/\gamma$). We also calculate from Eq. (15) the mean time of arrival to be $2610/\gamma$, that is in good agreement with Fig. 6. Note that here $\langle\gamma t\rangle > \sigma_t$ refers to a very good improvement of the resolution between the two circular components [$\gamma\delta\tau \ll \sigma_t$, as in Fig. 1(b)]. The value of the temporal separation obtained from Eq. (17) is then $\delta\tau = \frac{525}{\gamma}$ [33]. Thus, for a given β we can obtain $\langle t\rangle$ from Eq. (15) and thereby can obtain $\delta\tau$ by using Eq. (17).

We further investigate the effect of changing the width of the Gaussian pulse on the above-mentioned correspondence. By increasing the width in the frequency domain ($\sigma = 2\pi \times 7.916$ kHz), we found that the linearity between $2\langle\gamma t\rangle$ and $\gamma\delta\tau$ is still maintained [see Fig. 7].

We find that a similar correspondence between $\langle t\rangle$ and $\delta\tau$ can be obtained in alkali atoms in a tripod configuration [32], as well. Note that such a configuration is known to work as a polarization splitter of pulses.

Next, we discuss how this correspondence can be useful to obtain the number density N of the medium. The time t_- (t_+) taken by the σ_- (σ_+) component of the pulse to reach the detector is related to the DGD by $\delta\tau = t_- - t_+ = L/v_g^- - L/v_g^+$, where $v_g^\pm$ are the group velocities of $\sigma_\pm$ components inside the medium and are given by Eq. (A12). Using the values of $\chi_\pm$ [Eqs. (A10), (A11)], it can be easily shown that $\delta\tau \propto N$. Thus, we can get the value of N by calculating $\delta\tau$ from the above mentioned correspondence. It is to be noted that

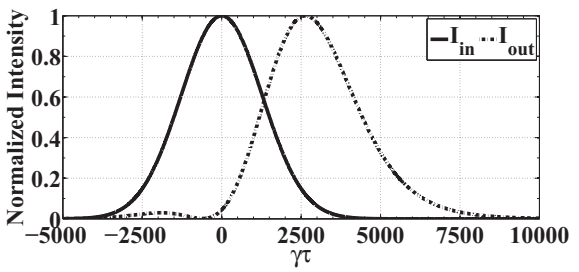

FIG. 6. The input Gaussian pulse (solid line) and the normalized output pulse (dot-dashed line). Here, $\beta = 0.1$ and the rest of the parameters used are the same as in Fig. 1. The output intensity of the probe pulse corresponds to 9.32 nW/cm^2 for an input intensity of 1 μW/cm^2.

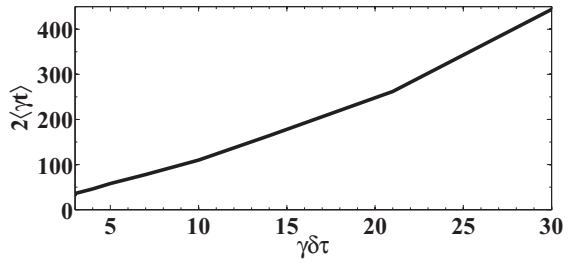

FIG. 7. The variation of $2\langle\gamma t\rangle$ with $\gamma\delta\tau$. Here, $\sigma = 2\pi \times 7.916$ kHz and the other parameters are the same as in Fig. 5.

N could be calculated by using the usual absorption method, in which the intensity of the input pulse gets reduced by a fraction $\xi = e^{-\alpha N}$ at the output. Here $\alpha = \frac{3L\lambda_{ij}^2}{2\pi}\mathrm{Im}[\rho_{ij}^{(1)}]$. However, the associated relative error can be written as

$$\left|\frac{dN}{N}\right| = \left|\frac{1}{N\alpha}\right|\left|\frac{d\xi}{\xi}\right|. \tag{18}$$

This implies that with a decrease in the number density, the relative error in the number density increases for the usual absorption procedure. In such a situation, when N is small (i.e., when the absorption of the pulse is negligible), the proposed method of measuring N using weak measurement would be much more useful.

E. Effect of absorption

The above results are discussed for negligible absorption of the polarization components of the input field. But, in the presence of substantial absorption, the weak value [Eq. (14)] can be written as

$$\mathrm{Re}W = \frac{[1+\cot(\beta)]^2 - \eta^2[1-\cot(\beta)]^2}{(1+\eta)^2\left[\cot^2(\beta)\sin^2\left(\frac{\omega_0\delta\tau}{2}\right)+\cos^2\left(\frac{\omega_0\delta\tau}{2}\right)\right]+(1-\eta)^2\left[\cot^2(\beta)\cos^2\left(\frac{\omega_0\delta\tau}{2}\right)+\sin^2\left(\frac{\omega_0\delta\tau}{2}\right)\right]+2(1-\eta^2)\cot(\beta)}, \tag{19}$$

where η gives the ratio of the electric field amplitude of the σ_- component relative to the σ_+ component. For equal absorption ($\eta = 1$), Eq. (19) reduces to Eq. (16). In the case of significant absorption of the σ_- component $\eta \ll 1$, Eq. (19) would give $\mathrm{Re}W = 1$. On the contrary, when $\eta \gg 1$, i.e., when the σ_+ polarized component gets absorbed, Eq. (19) would give $\mathrm{Re}W = -1$. In these situations, the medium would act as a polarizing medium. This puts a limitation on the weak measurement of the DGD in an atomic vapor system in the presence of large absorption.

III. CONCLUDING REMARKS

The measurement of temporal separation can be limited by several technical errors (e.g., the misalignment of the polarizers, the stability of laser pointing, the intensity resolution of the detector). Several schemes have been proposed to suppress these technical errors in Refs. [10,11,34–37]. For our scheme to work, the conditions to be obeyed are $\langle t\rangle > \Delta t$ and $\delta\tau \approx \Delta t$, where Δt is the temporal resolution of the detector. For a detector with $\Delta t = 1\mu$s, our proposal of measuring the DGD would work well even with an ordinary detector. However, for a detector with higher temporal resolution [38], the condition $\delta\tau \approx \Delta t$ demands that $\delta\tau$ is to be reduced. Further, measurement of the temporal separation can be limited by statistical errors, i.e., the total number of photons detected at the detector. The probability of successful postselection is given by $p = |\langle\psi_1|\psi\rangle|^2$. In the regime where the two polarizers are nearly orthogonal ($\beta \approx 0$), the intensity of the output pulse will be lowered ($I_{\mathrm{out}} = 0.298$ nW/cm^2). So, one needs to optimize for an appropriate value of β by considering the detector efficiency. However, the overall sensitivity can be increased by using standard signal modulation and lock-in detection techniques [6].

In conclusion, we have discussed the use of weak values of polarization in temporally resolving two overlapping circular polarization components of a weak linearly polarized pulse, propagating through a coherently driven alkali atomic vapor. We find that while a postselection would give rise to large weak value, the strong control field also plays a crucial role in obtaining a good temporal resolution. Such a control is inherently absent in experiments with photons passing through an optical fiber. We have shown that the temporal separation between the two polarization components can be obtained from the mean time of arrival of an output pulse in a postselected polarization. For negligible absorption, we obtain a linear relationship between this separation and the mean time, while in the case of absorption, they exhibit a nontrivial relation as a function of the control field Rabi frequency and the postselected basis. We have provided full analytical and numerical results to demonstrate the above idea.

ACKNOWLEDGMENT

One of us (S.D.) gratefully acknowledges Prof. G. S. Agarwal, who originally proposed the idea.

APPENDIX

We choose a generic four-level configuration [39] as shown in Fig. 8. A dc magnetic field is applied to remove the degeneracy of the excited and the ground states. In general, the Zeeman separation $2B$ of the excited states ($|3\rangle$,$|4\rangle$) is not the same as the Zeeman separation $2B'$ of the ground manifolds ($|1\rangle$,$|2\rangle$), due to the difference in Landé g factors in these manifolds. For ^{39}K, $B' = 3B$, $g_e = 2/3$, and $g_g = 2$ are the Landé g factors of the excited and the ground sublevels. We consider the propagation of an $\hat{x}$-polarized probe pulse [Eq. (3)] through the atomic medium. The $\sigma_\pm$ components of this probe pulse interact with the transitions $|2\rangle \leftrightarrow |3\rangle$ and $|1\rangle \leftrightarrow |4\rangle$, respectively. The corresponding Rabi frequencies are given by $2g_+ = 2(\frac{\vec{d}_{32}\cdot\hat{x}\varepsilon_p}{\hbar})$ and $2g_- = 2(\frac{\vec{d}_{41}\cdot\hat{x}\varepsilon_p}{\hbar})$, where $\vec{d}_{ij}$ is the electric dipole moment matrix element between the levels $|i\rangle$ and $|j\rangle$. A strong π-polarized control field is applied to drive the transitions $|1\rangle \leftrightarrow |3\rangle$ and $|2\rangle \leftrightarrow |4\rangle$. The Rabi frequency of this control field is given by $2G = 2(\frac{\vec{d}_{31}\cdot\hat{z}\varepsilon_p}{\hbar}) = 2(\frac{\vec{d}_{42}\cdot\hat{z}\varepsilon_c}{\hbar})$.

The Hamiltonian for the above configuration can be written in the dipole approximation as

$$\begin{aligned}\hat{H} &= \hbar[\omega_{21}|2\rangle\langle 2| + \omega_{31}|3\rangle\langle 3| + \omega_{41}|4\rangle\langle 4|] \\ &\quad - [(\vec{d}_{41}|4\rangle\langle 1| + \vec{d}_{32}|3\rangle\langle 2| + \text{H.c.}) \cdot \vec{E}_p] \\ &\quad - [(\vec{d}_{31}|3\rangle\langle 1| + \vec{d}_{42}|4\rangle\langle 2| + \text{H.c.}) \cdot \vec{E}_c]. \end{aligned} \tag{A1}$$

Here zero of energy is defined at the level $|1\rangle$ and $\hbar\omega_{\alpha\beta}$ is the energy difference between the levels $|\alpha\rangle$ and $|\beta\rangle$. Including the natural decay terms into our analysis and using the Markovian master equation under rotating wave approximation, the following density matrix equations are obtained:

$$\begin{aligned}
\dot{\tilde{\rho}}_{11} &= \gamma_{13}\tilde{\rho}_{33} + \gamma_{14}\tilde{\rho}_{44} + i(G^*\tilde{\rho}_{31} - G\tilde{\rho}_{13}) + i(g_+^*\tilde{\rho}_{41}e^{i\omega_{pc}t} - g_+\tilde{\rho}_{14}e^{-i\omega_{pc}t}), \\
\dot{\tilde{\rho}}_{33} &= -(\gamma_{13} + \gamma_{23})\tilde{\rho}_{33} + i(G\tilde{\rho}_{13} - G^*\tilde{\rho}_{31}) + i(g_-\tilde{\rho}_{23}e^{-i\omega_{pc}t} - g_-^*\tilde{\rho}_{32}e^{i\omega_{pc}t}), \\
\dot{\tilde{\rho}}_{44} &= -(\gamma_{14} + \gamma_{24})\tilde{\rho}_{44} + i(G\tilde{\rho}_{24} - G^*\tilde{\rho}_{42}) + i(g_+\tilde{\rho}_{14}e^{-i\omega_{pc}t} - g_+^*\tilde{\rho}_{41}e^{i\omega_{pc}t}), \\
\dot{\tilde{\rho}}_{31} &= i(\Delta - 2B + 2B' + +i\Gamma_{31})\tilde{\rho}_{31} + i(\tilde{\rho}_{11} - \tilde{\rho}_{33})G + i(g_-\tilde{\rho}_{21} - g_+\tilde{\rho}_{34})e^{-i\omega_{pc}t}, \\
\dot{\tilde{\rho}}_{32} &= i(\Delta - 2B + i\Gamma_{32})\tilde{\rho}_{32} + i(\tilde{\rho}_{12} - \tilde{\rho}_{34})G + i(1 - \tilde{\rho}_{11} - 2\tilde{\rho}_{33} - \tilde{\rho}_{44})g_-e^{-i\omega_{pc}t}, \\
\dot{\tilde{\rho}}_{43} &= (2iB - \Gamma_{43})\tilde{\rho}_{43} + i(G\tilde{\rho}_{23} - G^*\tilde{\rho}_{41}) + i(g_+\tilde{\rho}_{13}e^{-i\omega_{pc}t} - g_-^*\tilde{\rho}_{42}e^{i\omega_{pc}t}), \\
\dot{\tilde{\rho}}_{42} &= i(\Delta + i\Gamma_{42})\tilde{\rho}_{42} + i(1 - \tilde{\rho}_{11} - \tilde{\rho}_{33} - 2\tilde{\rho}_{44})G + i(g_+\tilde{\rho}_{12} - g_-\tilde{\rho}_{43})e^{-i\omega_{pc}t}, \\
\dot{\tilde{\rho}}_{41} &= i(\Delta + 2B' + i\Gamma_{41})\tilde{\rho}_{41} + i(\tilde{\rho}_{21} - \tilde{\rho}_{43})G + i(\tilde{\rho}_{11} - \tilde{\rho}_{44})g_+e^{-i\omega_{pc}t}, \\
\dot{\tilde{\rho}}_{21} &= (2iB' - \Gamma_{21})\tilde{\rho}_{21} + i(G^*\tilde{\rho}_{41} - G\tilde{\rho}_{23}) + i(g_-^*\tilde{\rho}_{31}e^{i\omega_{pc}t} - g_+\tilde{\rho}_{24}e^{-i\omega_{pc}t}),
\end{aligned} \tag{A2}$$

where $\Delta = \omega_c - \omega_{42}$ is the control field detuning from the transition $|2\rangle \leftrightarrow |4\rangle$, $\delta = \omega_p - \omega_{41}$ is the probe detuning from the transition $|1\rangle \leftrightarrow |4\rangle$, and $\omega_{pc} = \delta - \Delta - 2B'$ is the probe-pump detuning. γ_{ij} is the spontaneous emission rate from the level $|j\rangle$ to $|i\rangle$, $\Gamma_{ij} = \frac{1}{2}\sum_k(\gamma_{ki} + \gamma_{kj}) + \gamma_{\text{coll}}$ is the dephasing rate of the coherence between the levels $|j\rangle$ and $|i\rangle$, and γ_{coll} is the collisional decay rate. The transformations for the density matrix elements are as follows: $\rho_{31} = \tilde{\rho}_{31}e^{-i\omega_c t}$, $\rho_{32} = \tilde{\rho}_{32}e^{-i\omega_c t}$, $\rho_{42} = \tilde{\rho}_{42}e^{-i\omega_c t}$, and $\rho_{41} = \tilde{\rho}_{41}e^{-i\omega_c t}$. The rest of the elements remain the same.

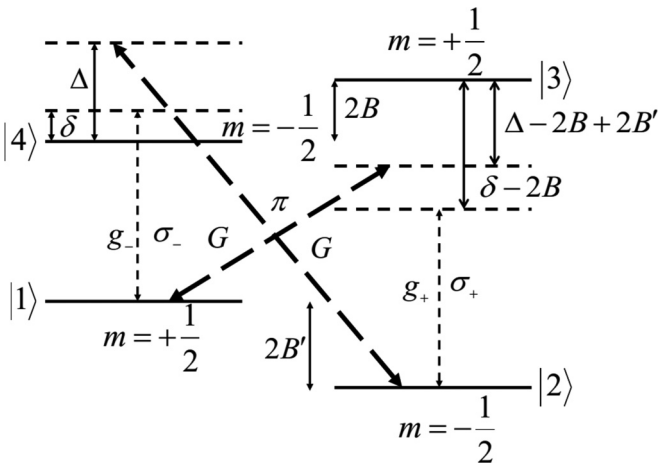

FIG. 8. Schematic energy-level structure of a four-level atomic system involving the $J = \frac{1}{2} \leftrightarrow J = \frac{1}{2}$ transition. The level $|4\rangle$ ($|3\rangle$) is coupled to the $|1\rangle$ ($|2\rangle$) by the σ_- (σ_+) component of the probe pulse with the Rabi frequency g_- (g_+). A π-polarized control field couples the level $|4\rangle$ ($|3\rangle$) to the $|2\rangle$ ($|1\rangle$). The detuning of the σ_- component from the respective transition is δ and the pumping field detuning is Δ. The degeneracy of the excited states $|4\rangle$, $|3\rangle$ and the ground sublevels $|1\rangle$, $|2\rangle$ have been removed by applying a dc magnetic field, so as to make the system anisotropic. The corresponding Zeeman separations are $2B$ and $2B'$, respectively.

The steady state solutions of Eq. (A2) can be found by expanding the density matrix elements in terms of the harmonics of ω_{pc} as

$$\begin{aligned}\tilde{\rho}_{\alpha\beta} &= \tilde{\rho}_{\alpha\beta}^{(0)} + g_+e^{-i\omega_{pc}t}\tilde{\rho}_{\alpha\beta}^{\prime(-1)} + g_+^*e^{i\omega_{pc}t}\tilde{\rho}_{\alpha\beta}^{\prime\prime(-1)} \\ &\quad + g_-e^{-i\omega_{pc}t}\tilde{\rho}_{\alpha\beta}^{\prime(+1)} + g_-^*e^{i\omega_{pc}t}\tilde{\rho}_{\alpha\beta}^{\prime\prime(+1)}. \end{aligned} \tag{A3}$$

Thus, we obtain a set of algebraic equations of $\tilde{\rho}_{\alpha\beta}^{(n)}$. These equations can be solved for different values of n to obtain following zeroth order solutions:

$$\begin{aligned}
\tilde{\rho}_{33}^{(0)} &= \frac{xy|G|^2\gamma_{14}}{Q}, \\
\tilde{\rho}_{44}^{(0)} &= \frac{xy|G|^2\gamma_{23}}{Q}, \\
\tilde{\rho}_{11}^{(0)} &= \frac{x}{Q}\gamma_{14}(\gamma_{13} + \gamma_{23} + y|G|^2), \\
\tilde{\rho}_{22}^{(0)} &= \frac{y}{Q}\gamma_{23}(\gamma_{14} + \gamma_{24} + x|G|^2), \\
\tilde{\rho}_{13}^{(0)} &= \frac{iG^*}{d_1^*}\frac{x\gamma_{14}}{Q}(\gamma_{13} + \gamma_{23}), \\
\tilde{\rho}_{24}^{(0)} &= \frac{iG^*}{d_2^*}\frac{y\gamma_{23}}{Q}(\gamma_{14} + \gamma_{24}),
\end{aligned} \tag{A4}$$

where

$$d_1 = i(\Delta - 2B + 2B') - \Gamma_{31}, \quad d_2 = i\Delta - \Gamma_{42}, \quad x = \frac{2\Gamma_{42}}{|d_2|^2}, \tag{A5}$$

$$y = \frac{2\Gamma_{31}}{|d_1|^2}, \quad Q = \gamma_{23}(\gamma_{14} + \gamma_{24})y + \gamma_{14}(\gamma_{13} + \gamma_{23})x + 2xy|G|^2(\gamma_{14} + \gamma_{23}).$$

Thus, the probe coherence terms for the $\sigma_{\pm}$ components can be written as

$$\tilde{\rho}_{41}^{\prime(-1)} = A_1 + B_1 + C_1, \tag{A6}$$

$$\tilde{\rho}_{32}^{\prime(+1)} = A_2 + B_2 + C_2, \tag{A7}$$

where

$$\begin{aligned}
A_1 &= \frac{-i[qrs + (q+r)|G|^2]\left(\tilde{\rho}_{11}^{(0)} - \tilde{\rho}_{44}^{(0)}\right)}{[pqrs + |G|^2(p+s)(q+r)]}, \\
B_1 &= \frac{rsG\tilde{\rho}_{24}^{(0)}}{[pqrs + |G|^2(p+s)(q+r)]}, \\
C_1 &= \frac{qsG\tilde{\rho}_{13}^{(0)}}{[pqrs + |G|^2(p+s)(q+r)]}, \\
A_2 &= \frac{-i[uvw + (v+u)|G|^2]\left(\tilde{\rho}_{22}^{(0)} - \tilde{\rho}_{33}^{(0)}\right)}{[fuvw + |G|^2(f+w)(u+v)]}, \\
B_2 &= \frac{vwG\tilde{\rho}_{13}^{(0)}}{[fuvw + |G|^2(f+w)(u+v)]}, \\
C_2 &= \frac{uwG\tilde{\rho}_{24}^{(0)}}{[fuvw + |G|^2(f+w)(u+v)]},
\end{aligned} \tag{A8}$$

with

$$\begin{aligned}
p &= i(\omega_{pc} + \Delta + 2B') - \Gamma_{41}, \quad q = i(\omega_{pc} + 2B') - \Gamma_{21}, \\
r &= i(\omega_{pc} + 2B) - \Gamma_{43}, \quad s = i(\omega_{pc} - \Delta + 2B) - \Gamma_{32}, \\
f &= i(\omega_{pc} + \Delta - 2B) - \Gamma_{32}, \quad u = i(\omega_{pc} - 2B') - \Gamma_{21}, \\
v &= i(\omega_{pc} - 2B) - \Gamma_{43}, \quad w = i(\omega_{pc} - \Delta - 2B') - \Gamma_{41}.
\end{aligned} \tag{A9}$$

The susceptibilities of the medium for the $\sigma_{\pm}$ components can be written as

$$\chi_{+} = \left(\frac{N|d_{32}|^2}{\hbar\gamma}\right)\tilde{\rho}_{32}^{\prime(+1)}, \tag{A10}$$

$$\chi_{-} = \left(\frac{N|d_{41}|^2}{\hbar\gamma}\right)\tilde{\rho}_{41}^{\prime(-1)}. \tag{A11}$$

The circularly polarized components of the pulse travel with different group velocities inside the medium which are given by

$$\begin{aligned}
v_g^{\pm} &= \frac{c}{n_g^{\pm}} \\
&= \frac{c}{\left[1 + 2\pi \mathrm{Re}[\chi_{\pm}(\omega)] + 2\pi\omega\frac{\partial}{\partial\omega}\mathrm{Re}[\chi_{\pm}(\omega)]\right]_{\omega=\omega_0}}.
\end{aligned} \tag{A12}$$

[1] Y. Aharonov, D. Z. Albert, and L. Vaidman, How the result of a measurement of a component of the spin of a spin-$\frac{1}{2}$ particle can turn out to be 100, Phys. Rev. Lett. **60**, 1351 (1988).

[2] Y. Aharonov and L. Vaidman, Aharonov and Vaidman reply, Phys. Rev. Lett. **62**, 2327 (1989).

[3] I. M. Duck, P. M. Stevenson, and E. C. G. Sudarshan, The sense in which a weak measurement of a spin-$\frac{1}{2}$ particle's spin component yields a value 100, Phys. Rev. D **40**, 2112 (1989).

[4] Y. Aharonov and L. Vaidman, Properties of a quantum system during the time interval between two measurements, Phys. Rev. A **41**, 11 (1990).

[5] N. W. M. Ritchie, J. G. Story, and R. G. Hulet, Realization of a measurement of a weak value, Phys. Rev. Lett. **66**, 1107 (1991).

[6] O. Hoston and P. Kwiat, Observation of the spin Hall effect of light via weak measurements, Science **319**, 787 (2008).

[7] P. B. Dixon, D. J. Starling, A. N. Jordan, and J. C. Howell, Ultrasensitive beam deflection measurement via interferometric weak value amplification, Phys. Rev. Lett. **102**, 173601 (2009).

[8] D. J. Starling, P. B. Dixon, A. N. Jordan, and J. C. Howell, Precision frequency measurements with interferometric weak values, Phys. Rev. A **82**, 063822 (2010).

[9] D. J. Starling, P. B. Dixon, A. N. Jordan, and J. C. Howell, Continuous phase amplification with a Sagnac interferometer, Phys. Rev. A **82**, 011802(R) (2010).

[10] N. Brunner and C. Simon, Measuring small longitudinal phase shifts: weak measurement or standard interferometry?, Phys. Rev. Lett. **105**, 010405 (2010).

[11] G. Strübi and C. Bruder, Measuring ultrasmall time delays of light by joint weak measurements, Phys. Rev. Lett. **110**, 083605 (2013).

[12] P. Egan and J. A. Stone, Weak value thermostat with 0.2 mK precision, Opt. Lett. **37**, 4991 (2012).

[13] J. S. Lundeen, B. Sutherland, A. Patel, C. Stewart, and C. Bamber, Direct measurement of the quantum wavefunction, Nature (London) **474**, 188 (2011).

[14] J. S. Lundeen and C. Bamber, Procedure for direct measurement of general quantum states using weak measurement, Phys. Rev. Lett. **108**, 070402 (2012).

[15] J. S. Lundeen and C. Bamber, Observing Dirac's classical phase space analog to the quantum state, Phys. Rev. Lett. **112**, 070405 (2014).

[16] J. Dressel, M. Malik, F. M. Miatto, A. N. Jordan, and R. W. Boyd, Colloquium: Understanding quantum weak values: Basics and applications, Rev. Mod. Phys. **86**, 307 (2014).

[17] N. S. Williams and A. N. Jordan, Weak values and the Leggett-Garg inequality in solid-state qubits, Phys. Rev. Lett. **100**, 026804 (2008).

[18] A. Romito, Y. Gefen, and Y. M. Blanter, Weak values of electron spin in a double quantum dot, Phys. Rev. Lett. **100**, 056801 (2008).

[19] G. S. Agarwal and P. K. Pathak, Realization of quantum-mechanical weak values of observables using entangled photons, Phys. Rev. A **75**, 032108 (2007).

[20] C. Hill and J. Ralph, Weak measurement and control of entanglement generation, Phys. Rev. A **77**, 014305 (2008).

[21] C. Simon and E. S. Polzik, Fock-state view of weak-value measurements and implementation with photons and atomic ensembles, Phys. Rev. A **83**, 040101(R) (2011).

[22] S. E. Ahnert and M. C. Payne, Weak measurement of the arrival time of single photons and pairs of entangled photons, Phys. Rev. A **69**, 042103 (2004).

[23] G. J. Pryde, J. L. O'Brein, A. G. White, T. C. Ralph, and H. M. Wiseman, Measurement of quantum weak values of photon polarization, Phys. Rev. Lett. **94**, 220405 (2005).

[24] Q. Wang, F. W. Sun, Y. S. Zhang, J. Li, Y. F. Huang, and G. C. Guo, Experimental demonstration of a method to realize weak measurement of the arrival time of a single photon, Phys. Rev. A **73**, 023814 (2006).

[25] J. C. Howell, D. J. Starling, P. B. Dixon, P. K. Vudyasetu, and A. N. Jordan, Interferometric weak value deflections: Quantum and classical treatments, Phys. Rev. A **81**, 033813 (2010).

[26] D. Rohrlich and Y. Aharonov, Cherenkov radiation of superluminal particles, Phys. Rev. A **66**, 042102 (2002).

[27] D. R. Solli, C. F. McCormick, R. Y. Chiao, S. Popescu, and J. M. Hickmann, Fast light, slow light, and phase singularities: A connection to generalized weak values, Phys. Rev. Lett. **92**, 043601 (2004).

[28] N. Brunner, V. Scarani, M. Wegmuller, M. Legre, and N. Gisin, Direct measurement of superluminal group velocity and signal velocity in an optical fiber, Phys. Rev. Lett. **93**, 203902 (2004).

[29] N. Brunner, A. Acin, D. Collins, N. Gisin, and V. Scarani, Optical telecom networks as weak quantum measurements with postselection, Phys. Rev. Lett. **91**, 180402 (2003).

[30] I. Shomroni, O. Bechler, S. Rosenblum, and B. Dayan, Demonstration of weak measurement based on atomic spontaneous emission, Phys. Rev. Lett. **111**, 023604 (2013).

[31] L. Zhou, Y. Turek, C. P. Sun, and F. Nori, Weak-value amplification of light deflection by a dark atomic ensemble, Phys. Rev. A **88**, 053815 (2013).

[32] G. S. Agarwal and S. Dasgupta, Coherent medium as a polarization splitter of pulses, Phys. Rev. A **65**, 053811 (2002).

[33] The disparity between the measured and the calculated values of $\gamma\delta\tau$ can be attributed to the non-Gaussian pulse shape at the output in Fig. 6.

[34] A. Feizpour, X. Xing, and A. M. Steinberg, Amplifying single-photon nonlinearity using weak measurements, Phys. Rev. Lett. **107**, 133603 (2011).

[35] D. J. Starling, P. B. Dixon, A. N. Jordan, and J. C. Howell, Optimizing the signal-to-noise ratio of a beam-deflection measurement with interferometric weak values, Phys. Rev. A **80**, 041803 (2009).

[36] A. Nishizawa, K. Nakamura, and M. K. Fujimoto, Weak-value amplification in a shot-noise-limited interferometer, Phys. Rev. A **85**, 062108 (2012).

[37] Y. Kedem, Using technical noise to increase the signal-to-noise ratio of measurements via imaginary weak values, Phys. Rev. A **85**, 060102 (2012).

[38] D. H. Sutter *et al.*, Semiconductor saturable-absorber mirror assisted Kerr-lens mode-locked Ti:sapphire laser producing pulses in the two-cycle regime, Opt. Lett. **24**, 631 (1999).

[39] P. Kumar and S. Dasgupta, Sharply tunable group velocity in alkali vapors using a single low-power control field, J. Phys. B: At. Mol. Opt. Phys. **47**, 175501 (2014).